Surfactant-Assisted Synthesis of $Ca_3(BTC)_2$ Metal-Organic Framework for the Removal of Heavy Metal

Wei Wang *, Ling-Li Liu , Shi-Yun Chen , Cheng-Liang Han , San-E Zhu

Posted Date: 12 January 2024

doi: 10.20944/preprints202401.0985.v1

Keywords: Metal-organic frameworks; Surfactant; ion-exchange; heavy metal; removal

Article

Surfactant-Assisted Synthesis of $Ca_3(BTC)_2$ Metal-Organic Framework for the Removal of Heavy Metal

Wei Wang [1,*], Ling-Li Liu [1], Shi-Yun Chen [2], Cheng-Liang Han [1] and San-E Zhu [1]

[1] School of Energy Materials and Chemical Engineering, Hefei University, 230601, China
[2] Analytical Instrumentation Center, Hefei University, Hefei 230601, China
* Correspondence: wangwei@hfuu.edu.cn

Abstract: Novel $Ca_3(BTC)_2$ metal-organic frameworks with different sizes and shapes constructed by Ca^{2+} and trimesic acid as metal center and ligands respectively were synthesized by a surfactant-assisted method. The relationship between the quantity of surfactant and the particle morphology of the product have been further studied. The samples were characterized by scanning electron microscope, powder X-ray diffraction and Inductively coupled plasma mass spectrometry. The results indicated that the size and shape of $Ca_3(BTC)_2$ could be regulated by changing the quantity of surfactant. Rod- and sheet-like $Ca_3(BTC)_2$ MOFs have been readily availabled. The removal kinetics of heavy metals of Pb(II) were also studied by rod-like $Ca_3(BTC)_2$. The results showed that as-synthesized $Ca_3(BTC)_2$ could effectively remove heavy metals of Pb(II) from the sewage.

Keywords: metal-organic frameworks; Surfactant; ion-exchange; heavy metal; removal

1. Introduction

Metal-organic frameworks (MOFs) are a very important new class of organic-inorganic hybrid compounds with porous and modular structures. MOFs consist of two parts: metal ion nodes or inorganic clusters, which are the secondary building units, as well as organically connected molecules or spacers. The various combinations of nodes and spacers, the flexibility with which their size, function, and geometry can be varied, all of these contribute to the preparation of large number of MOFs. Due to their extensive applications MOFs have attracted great interests in drug delivery, catalysis, optics, sensing, diagnosis, and storage[1]. In addition, the size of MOFs can be controlled at the nanoscale to generate nanoscale metal-organic frameworks (NMOFs). At the nanoscale level, Since the surface area to volume ratio of NMOF is larger, the proper connection of NMOF depends on its inner and outer surfaces. Hence, NMOF properties and behavior are considerably size and shape-dependent[2]. Depending on the synthetic process, NMOFs can exist in different forms to produce unique physicochemical properties. Small change in morphology can lead to changes in their properties.

Water contamination with heavy metals is one of the most serious environmental problems and causes global public health concerns. In the past few decades, great efforts have been attempted to minimize the impact of heavy metals in wastewater[3]. Currently, A number of techniques have been used to remove heavy metals from wastewater, such as adsorption, chemical precipitation, ion exchange, membrane filtration, electrolytic reduction, coagulation and so on[4–9]. Among them, ion-exchange is considered an efficient and facile method for wastewater treatment due to its many advantages, such as high processing capacity, high removal efficiency and fast kinetics. In addition, ion-exchange programs could not only remove dangerous metal ions, but also provide beneficial metal ions and even form some isomorphic frameworks[10,11]. In the materials used in the ion-exchange processes, synthetic resin[12,13], zeolites materials[14,15]and porous silicon[16,17]have been widely used to remove heavy metal from aqueous solutions. Due to the relatively low substitution efficiency of zeolite materials for heavy metals, porous materials with large surface area and

Preprints (www.preprints.org) | NOT PEER-REVIEWED | Posted: 12 January 2024 doi:10.20944/preprints202401.0985.v1

specificity have been used as metal concentrator to detect potential metal contaminated areas, making sample transportation and processing easier. However, compared to porous materials such as zeolites, active carbons and silicon mesoporous, MOFs have been investigated for the removal of heavy metal ions due to their more extremely adjustable pore structures and much higher porosities[18–20]. The characteristics of well defined pore shape and pore size mean that these frameworks have significant applications in the process of metal ion-exchange and adsorption[21,22].

It is an effective method to prepare nano or microcrystals for using surfactants as soft templates[23]. The crystals are generated within or around the limitary volume or space of the template. The growth and nucleation of nanoparticles or microcrystals can be limited by the spatially and dimensionally, just like in a reaction cage, resulting in the formation of nanoparticles with complementary morphology to the template. In addition, various morphologies of MOFs can be obtained by changing the shape and dosage of the template agent.

In our previous work, Hg^{2+} adsorption from water over thiol-functionalized Cu-BTC by a facile coordination based postsynthetic strategy have been reported [24]. The thiol-functionalized samples exhibited excellent adsorption capacityfor Hg^{2+} removal (714.29 mg g-1), while the exposed $[Cu_3(BTC)_2]n$ showed no adsorption of Hg^{2+} from the aqueous solution. To date, functionalization or grafting of MOFs based materials with different organic functional groups usually requires multiple steps to achieve selective removal of heavy metal ions from water. Compared to the large number of MOFs constructed from transition metal ions reported in the literature, the number of examples based on alkaline earth metals is relatively limited[25]. In addition, most MOFs as coordination polymers using transition metals, the secondary contamination during ion exchange may be induced, which improved the cost of sewage treatment.

Herein, not only a surfactant-assisted reaction of micro-sheets or micro-rods of MOFs $Ca_3(BTC)_2$ (BTC=1,3,5-benzenetricarboxylate) has been reported, but also the removal kinetics of heavy metals of Pb(II) was examined. The calcium-based MOF have an effective capture of Pb(II) through ion-exchange instead of adsorption. The rod-like $Ca_3(BTC)_2$ crystal is a two-dimensional (2D) layered calcium-BTC coordination polymer[26] which is synthesized by hydrothermal method. Significantly, the maximum removal capacities of $Ca_3(BTC)_2$ for Pb(II) is 555.6 mg/g. Clearly indicating that the $Ca_3(BTC)_2$ can be applied for selective removal of heavy metal ions from aqueous solution. The heavy metal ions exchange process of heavy metal ions was illustrated in Figure 1.

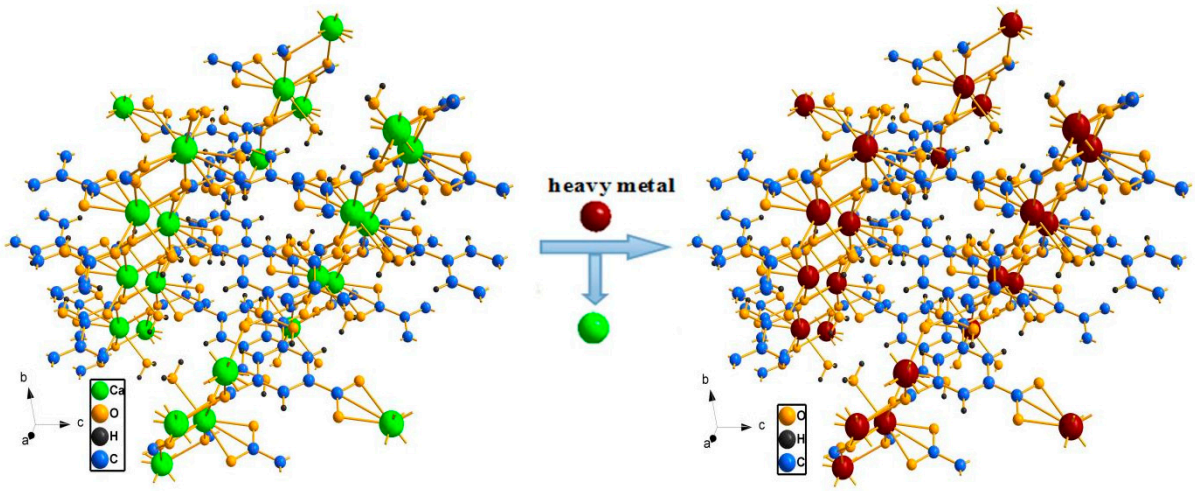

Figure 1. Schematic illustration of heavy metal ions exchange process of heavy metal ions.

 doi:10.20944/preprints202401.0985.v1

2. Experimental methods

2.1. Materials and methods

Benzene-1,3,5-tricarboxylic acid (H_3BTC) was purchased from Aldrich. Calcium acetate ($Ca(CH_3COO)_2$), lead chloride ($PbCl_2$), was purchased from Sinopharm (Shanghai) Chemical Reagent Co.Ltd. The water used in this experiment was deionized water. Other chemical reagents and organic solvents were analytical grade, obtained from commercial suppliers, and could be used without further purification. PXRD patterns of the samples were collected by using an X-ray diffractometer with Cu target (36 kV, 25 mA) from 5°to 40. The morphologies and size or nanostructure of the products were characterized on a SU8010 field emission scanning electron microscopy (FE-SEM) equipped with an energy dispersive X-ray (Oxford Instruments INCA EDX) system. The concentration values of metal ions (such as Ca^{2+}, Pb(II) were confirmed by the inductively coupled plasma mass spectrometer (ICP-MS, iCAPQ, Thermo Fisher, USA).

2.2. Synthesis of $Ca_3(BTC)_2$

$Ca_3(BTC)_2$ crystals were prepared by a hydrothermal method. 0.0316 g (0.2 mmol) $Ca(CH_3COO)_2$ was dissolved in deionized water(20 mL), and 0.042g(0.2 mmol) H_3BTC(BTC=benzene-1,3,5-tricarboxylate) and 2 mL absolute ethanol were simultaneously added into the above solution. The reaction mixture was vigorously stirred for 30 minutes to form a homogeneous solution, Then, different quantity (0.2 g，0.4 g，0.6 g，and 0.8 g) of CTAB were added and loaded into the Teflon autoclave. The autoclave was heated to 180°C for 10 h, then slowly cooled to 80°C for 36 h, and after that cooled to room temperature. The obtained white powder was filtered off, washed several times with deionized water and ethanol, and then dried at 70°C under air atmosphere overnight in drying oven.

2.3. Capture and selectivity of $Ca_3(BTC)_2$ for Pb(II)

The metal salt aqueous solutions of $PbCl_2$ with different concentrations were immersed in a solution of deionized water (25 mL). To demonstrate the ability of $Ca_3(BTC)_2$ for removal of Pb(II), the ion exchange between Ca^{2+} of $Ca_3(BTC)_2$ and Pb(II) was quantitatively analyzed by the inductively coupled plasma mass spectrometer experiment. The selectivity properties for Pb(II) was determined by adding 50 mg of $Ca_3(BTC)_2$ with 0.2g CTAB as template to 25 mL of the above solution at room temperature for 24h. The products were collected by centrifugation and the concentration of the supernatant was measured by ICP-MS.

3. Results and discussion

3.1. Measurement of $Ca_3(BTC)_2$ samples before and after ion-exchange

Structure of as-synthesized $Ca_3(BTC)_2$ sample was primarily characterized by PXRD. The PXRD pattern of as-synthesized sample and the simulated pattern of $Ca_3(BTC)_2$ are shown in Figure 2. And the suface profile of $Ca_3(BTC)_2$ was measured by Scanning Electron Microscope (SEM). As can be seen from Figure 2, compared with the simulated $Ca_3(BTC)_2$ XRD patterns from its crystal structural data, all peaks from the resulting $Ca_3(BTC)_2$ crystals are preserved, suggesting that this pattern is in agreement with the simulated $Ca_3(BTC)_2$ XRD patterns[27].

XRD analysis of the MOFs for different quantity of CTAB was characterized (Figure 2). As revealed by XRD, all of the diffraction peaks for the synthesized $Ca_3(BTC)_2$ can be readily indexed to the simulated pattern of $Ca_3(BTC)_2$.

Preprints (www.preprints.org) | NOT PEER-REVIEWED | Posted: 12 January 2024 doi:10.20944/preprints202401.0985.v1

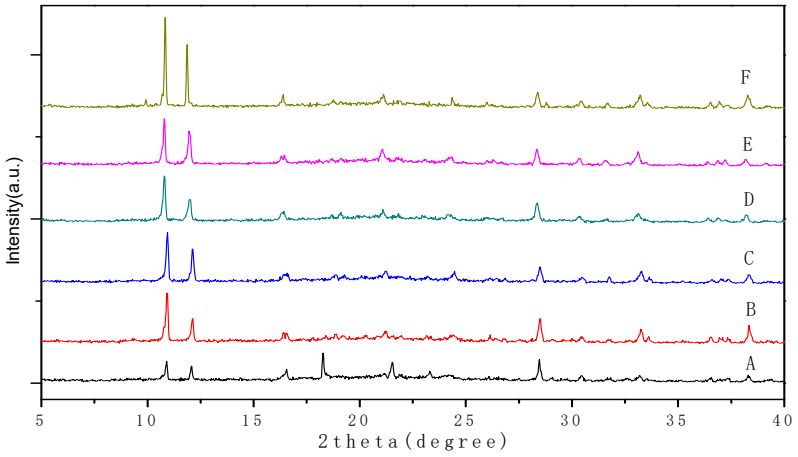

Figure 2. PXRD of $Ca_3(BTC)_2$, synthesized for different quantity of CTAB: (A) 0 g, (B) 0.2 g, (C) 0.4 g, (D) 0.6 g, (E) 0.8 g and (F) simulated $Ca_3(BTC)_2$.

The morphology and size of samples prepared with different quantity of CTAB were comprehensively characterized by SEM (Figure 3). SEM images show that $Ca_3(BTC)_2$ is sheet-like or rod-like, with a width is of approximately 1 μm and a length of 5 μm. The material morphology depends on the quantity of the CTAB added.

In the absence of CTAB, the synthesized material is blocky and about 5 μm in length. As the quantity of CTAB increased to 0.2g, a few of microrods with pores on the surface were formed (Figure 3b). As the quantity of CTAB increased to 0.4g, some microsheets were formed (Figure 3c). With improving the quantity of CTAB from 0.4-0.6 g, more and more regular micro-rods have emerged(Figure 3d). The continuous increase in the quantity of CTAB to 0.8g leads to the generation of regular microrods (Figure 3e). These results show that the the addition of CTAB is critical for the final morphology and size, Therefore, it is reasonable to speculate that CTAB plays an important role in controlling the size and morphology of Ca-MOFs. In addition, the morphology of $Ca_3(BTC)_2$ after ion exchange with Pb(II) has also been studied. The results showed that the morphology of the materials changed greatly after ion exchange (Figure 3f)， due to ion exchange, the morphology of the product changed from rod-shaped to sheet-shaped, the exchange process is further verified.

Preprints (www.preprints.org) | NOT PEER-REVIEWED | Posted: 12 January 2024 doi:10.20944/preprints202401.0985.v1

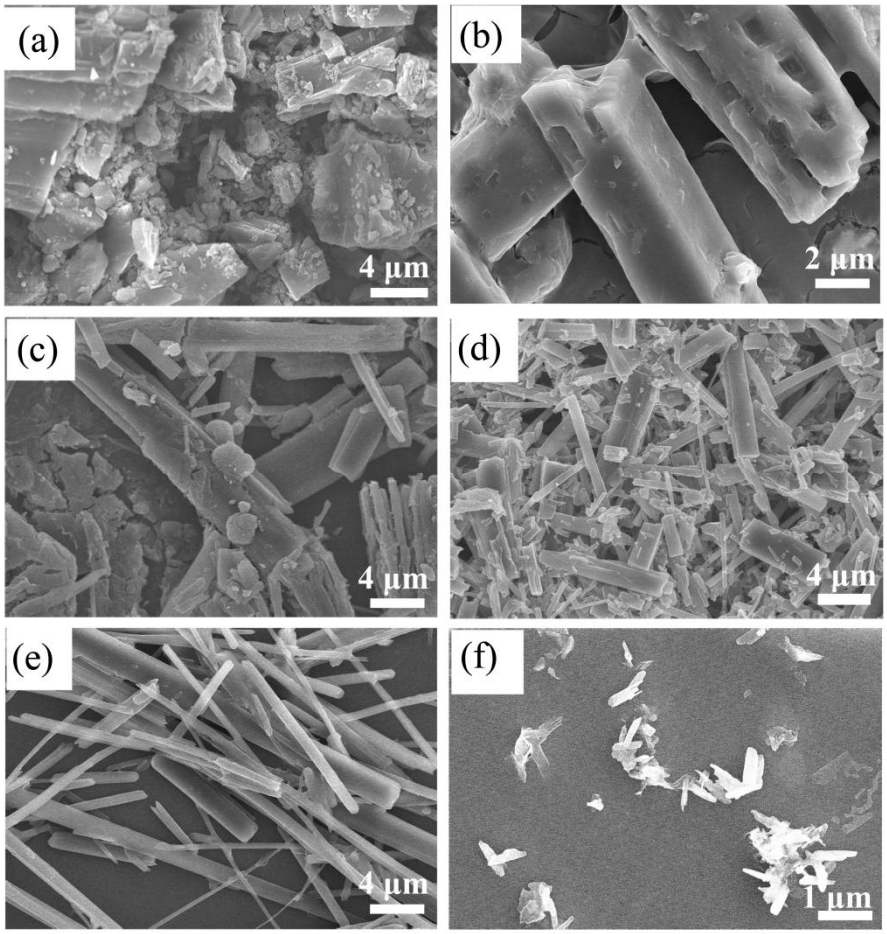

Figure 3. SEM images, synthesized for different quantity of CTAB: (a) 0 g, (b) 0.2 g, (c) 0.4 g, (d) 0.6 g and (e) 0.8g; (f) $Ca_3(BTC)_2$ ion exchange with Pb(II) at 24h.

To confirm the process of ion exchange, the metal ion exchange process of heavy metals by Energy Dispersive Spectrometer(EDX) was followed (Figure 4). The EDX images showed that Ca^{2+} in Ca-MOF was completely exchanged with Pb(II) in solution after 24 hours of reaction (Figure 4d). The main reason is that the coordination ability between Ca^{2+} and H_3BTC is lower than that of Pb(II), Pb(II) will seize some organic functional groups, leading to partial crystal dissolution, and the dissolved composite anions interact with Pb(II) to form composite precipitates. With the progress of the reaction, an increasing number of organic functional groups were complexed with Pb(II) to form three-dimensional solid materials. Due to the reaction conditions at room temperature and atmospheric pressure, the resulting heavy metal complexes were not three-dimensional ordered crystals with uniform size, but rather disordered solid materials.

 doi:10.20944/preprints202401.0985.v1

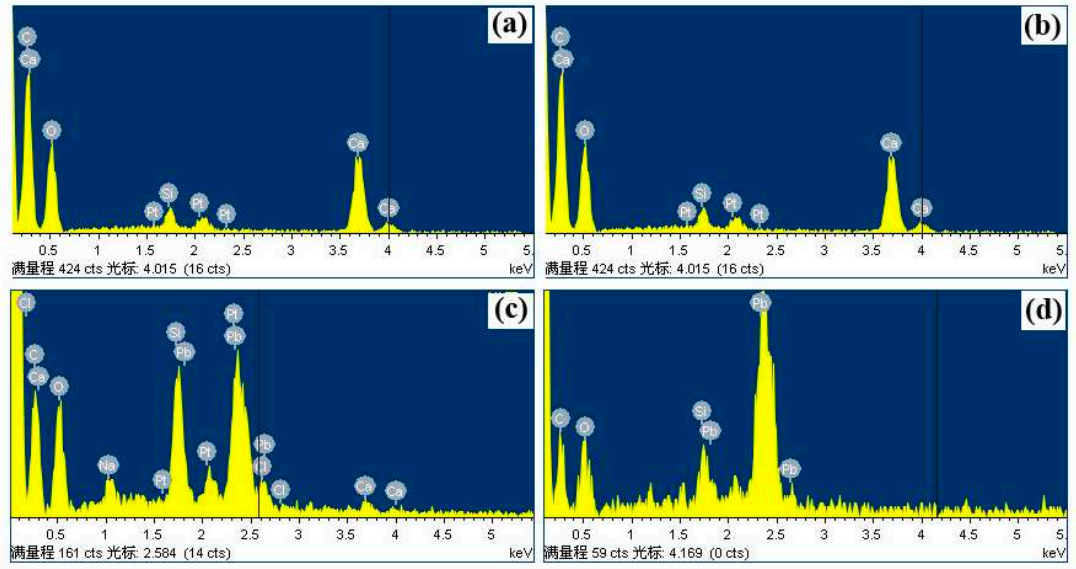

Figure 4. EDX images, (a) $Ca_3(BTC)_2$, (b) $Ca_3(BTC)_2$ synthesized for 0.2 g CTAB. (c) $Ca_3(BTC)_2$ ion exchange with Pb(II) at 3 h, (d) $Ca_3(BTC)_2$ ion exchange with Pb(II) at 24 h.

3.2. Adsorption isotherms for Pb(II)

The adsorption isotherm was used to better understand the mechanism on heavy metal removal, as shown in Figure 5. The capture capacities of Pb(II) increases rapidly at lower Pb(II) concentration (less than 7.81 mg/L). When the concentration of Pb(II) is higher than this value, further increases in Pb(II) concentration will not enhance the capture capacity of Pb(II). These experimental results indicate the saturated exchange capacity of Pb(II) on $Ca_3(BTC)_2$ is approximately 530.8 mg/L. The maximum exchange capacity of Pb(II) was estimated by fitting the equilibrium capture data with the Langmuir adsorption model, which can be described as[28–30]:

$$Ce/qe = Ce/qm + 1/qmKL$$

where Ce(mg/L) is the equilibrium concentration of remaining Pb(II) in the solution, qe(mg/g) is the equilibrium exchange capacity, which is the displacement Pb(II) per mass unit of Ca-MOF at equilibrium, qm is the saturation capacity of Ca-MOF and KL(L/mg) is the Langmuir constant.

The linear regression between Ce/qe and Ce was calculated, as shown in Figure 5b. The correlation coefficient is 0.9958, it is shown that the capture of Pb(II) is well followed by Langmuir adsorption model. The saturation capacity for the capture of Pb(II) is determined to be 555.6 mg/g by fitting the equilibrium capture data with the Langmuir adsorption model (see Figure 5). It is notable that the maximum capacity of the material obtained here is much greater than the maximum capacity of many other porous materials[31–34].

Preprints (www.preprints.org) | NOT PEER-REVIEWED | Posted: 12 January 2024 doi:10.20944/preprints202401.0985.v1

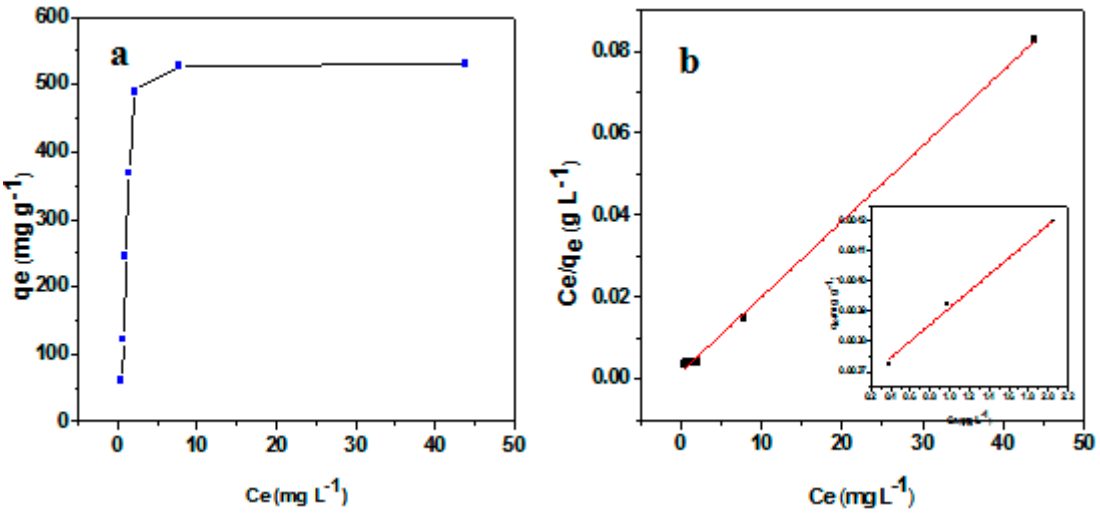

Figure 5. (a) Capture curve of $Ca_3(BTC)_2$ at different concentration of Pb(II). (b) The linear regression by fitting the equilibrium adsorption data with the Langmuir adsorption model; The illustration shows the liner regression of the Langmuir adsorption model at low concentration of Pb(II) .

3.3. Adsorption kinetics

To evaluate the adsorption kinetics, the adsorption kinetics of $Ca_3(BTC)_2$ on Pb(II) were studied. As the concentration of Pb(II) increases, the growth rate of Ca^{2+} slows down, indicates that the exchange capacities of Pb(II) tended to achieve the maximum after 20h (1200min), and almost 86% of Pb(II) was replaced by Ca^{2+} from the framework within 20h. (see Figure 6). All the exchange was observed by ICP-MS analysis. It can be observed that the removal efficiency of Ca^{2+} is relatively high in all cases.

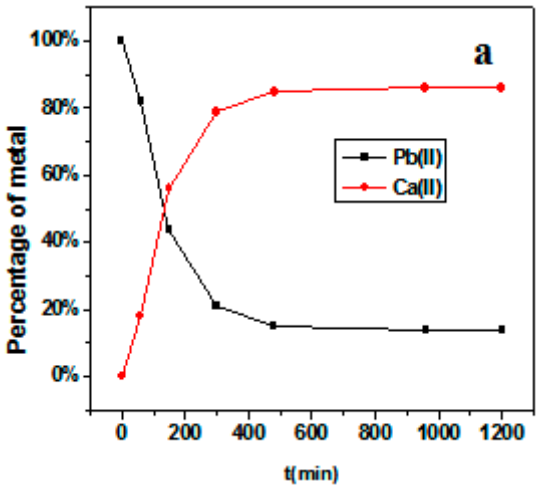

Figure 6. (a) Kinetic profiles of Pb (II) and Ca (II) metal ion exchange of $Ca_3(BTC)_2$.

4. Conclusions

In this paper, a facile approach for the removal of heavy metal ions through bare $Ca_3(BTC)_2$. Pb(II) can be replaced by Ca^{2+} of $Ca_3(BTC)_2$ efficiently. $Ca_3(BTC)_2$ material exhibited excellent capture ability for Pb(II). During the ion-exchange process, the materials not only exhibit different topological structures, but also showed extremely high removal ability for Pb(II), reaching 555.6 mg g^{-1}. In addition, the Ca-MOF exhibited high adsorption affinity and the Kd value was calculated to be 1.97×10^3 for Pb(II). Due to the process involves the replacement between heavy metal ions and Ca^{2+} of $Ca_3(BTC)_2$, the cation size and coordination abilities of metal ions play an important role in the

facile ion exchange process. In summary, this work provides a green and facile method for selective removal of heavy metal ions by Ca-MOF, and even provides a synthesis method for heterostructure materials including different MOFs.

Acknowledgements: Wei-Wang is grateful for Key projects of Anhui Provincial Department of Education (2023AH052195) and Supported by Support Project for the Outstanding Young Talents of Higher Learning Institutions of Anhui (gxyq2022073).

References

1. X.Y. Shi, Y.Y. Shan, M. Du, et al. Synthesis and application of metal-organic framework films. Coord. Chem. Rev., 444 (2021) 214060.
2. P. Hirschle, T. Preiß, F. Auras, et al. Exploration of MOF nanoparticles sizes using various physical characterization methods-is what you measure what you get. Cryst. Eng. Comm., 18 (2016) 4359-4368.
3. B.J. Zhu, X.Y. Yu, Y. Jia. Iron and 1,3,5-Benzenetricarboxylic Metal–Organic Coordination Polymers Prepared by Solvothermal Method and Their Application in Efficient As(V) Removal from Aqueous Solutions. Phys. Chem., 116 (2012) 8601-8607.
4. N.A. Khan, Z. Hasan, S.H. Jhung. Adsorptive Removal of Hazardous Materials Using Metal-Organic Frameworks (MOFs): A Review. J. Hazard. Mater., 244-245 (2013) 444-456.
5. F. L.Fu, L.P. Xie, B. Tang, et al. Application of a novel strategy-Advanced Fenton-chemical precipitation to the treatment of strong stability chelated heavy metal containing wastewater. Chem. Eng. J., 189-190 (2012) 283-287.
6. G. Sharma, B. Thakur, M. Naushad, et al. Fabrication and characterization of sodium dodecyl sulphate@ironsilicophosphate nanocomposite: Ion exchange properties and selectivity for binary metal ions. Mater. Chem. Phys., 193 (2017) 129-139.
7. J. Song, H. Oh, H. Kong, et al. Polyrhodanine modified anodic aluminum oxide membrane for heavy metal ions removal. J. Hazard. Mater.,187(2011) 311-317.
8. R.T. Brosky, S. Pamukcu. Role of DDL processes during electrolytic reduction of Cu(II) in a low oxygen environment. J. Hazard. Mater.,262 (2013) 878-882.
9. N. Hilal, M. Al-Abri, A. Moran, et al. Effects of heavy metals and polyelectrolytes in humic substance coagulation under saline conditions. Desalination 220 (2008) 85-95.
10. L.W. Mi, H.W. Hou, Z.Y. Song, et al. Polymeric Zinc Ferrocenyl Sulfonate as a Molecular Aspirator for the Removal of Toxic Metal Ions, Chem. Eur. J., 14(2008)1814-1821.
11. S. Das, H. Kim, K. Kim. Metathesis in single crystal: complete and reversible exchange of metal ions constituting the frameworks of metal-organic frameworks, J. Am. Chem. Soc., 131 (2009) 3814-3815.
12. N. Dizge, B. Keskinler, H. Barlas. Sorption of Ni(II) ions from aqueous solution by Lewatit cation-exchange resin[J]. J. Hazard. Mater., 167 (2009) 167915-167926.
13. C.H. Xiong, Y.J. Feng, C.P. Cai. Adsorption of Pb^{2+} on macroporous weak acid adsorbent resin from aqueous solutions: Batch and column studies. J. Cent. South Univ. Technol., 16 (2009): 569-574 .
14. S.B. Wang, Y..L. Peng, Natural zeolites as effective adsorbents in water and wastewater treatment. Chem. Eng. J., 156 (2010) 11-24.
15. E. Erdem, N. Karapinar, R. Donat. The removal of heavy metal cations by natural zeolites. J. Colloid Interface Sci., 280 (2004) 309-314.
16. R.F. Balderas-Valadez, M. Weiler, V. Agarwal, et al. Optical characterization of porous silicon monolayers decorated with hydrogel microspheres. Nano. Res. Lett., 9 (2014) 425-431.
17. E. Mery, S.A. Alekseev, V.N. Zaitsev, et al. Covalent grafting of ion-exchanging groups on porous silicon for microsystem applications. Sens. Actuators, B: Chem., 126 (2007) 120-125.
18. M. Plabst, L.B. McCusker, T. Bein. Exceptional Ion-Exchange Selectivity in a Flexible Open Framework Lanthanum(III)tetrakisphosphonate. J. Am. Chem. Soc., 131 (2009) 18112-18118.
19. H.H. Fei, J.F. Cahill, K.A. Prather, et al.Tandem Postsynthetic Metal Ion and Ligand Exchange in Zeolitic Imidazolate Frameworks. Inorg. Chem., 52 (2013) 4011-4016.
20. J. Canivet, A. Fateeva, Y. Guo, et al. Water adsorption in MOFs: fundamentals and Applications Farrusseng. Chem. Soc. Rev. 43 (2014) 5594-5617.

21. M. Kim, J.F. Cahill, H. Fei, et al. Postsynthetic Ligand and Cation Exchange in Robust Metal–Organic Frameworks. J. Am. Chem. Soc., 134 (2012) 18082-18088.
22. M. Shu, C.L. Tu, W.D. Xu, et al. Reversible Anion Exchanges of Porous Metal-Organic Frameworks: Syntheses and Structures of Silver Complexes with Novel Rigid Tripodal Nitrogen Ligands. Cryst. Growth Des., 6 (2006) 1890-1896.
23. P. S. Prasad, B. C. G. Marupalli, S. Das, et al. Surfactant-assisted synthesis of hydroxyapatite particles: a comprehensive review. J. Mater. Sci., 58 (2023): 6076-6105.
24. F. Ke, L.G. Qiu, Y.P. Yuan, et al. Thiol-functionalization of metal-organic framework by a facile coordination-based postsynthetic strategy and enhanced removal of Hg^{2+} from water. J. Hazard. Mater., 196 (2011) 36-43.
25. R.K. Vakiti, B.D. Garabato, N.P. Schiebe, et al. Synthesis and Characterization of Two- and Three-Dimensional Calcium Coordination Polymers Built with Benzene-1,3,5-tricarboxylate and/or Pyrazine-2-carboxylate, Cryst. Growth Des., 12 (2012) 3937-3943.
26. Y.Y. Yang, Z.Q. Huang, L. Szeto, et al. A two-dimensional layer structure containing calcium: [Ca_3(1,3,5-benzenetricarboxylate)$_2$(H_2O)$_{12}$]n. Appl. Organomet. Chem., 18 (2004) 97-98.
27. M.J. Platers, R. A. Howie, A.J. Roberts. Hydrothermal synthesis and X-ray structural characterisation of calcium benzene-1,3,5-tricarboxylate, Chem. Commun. 7 (1997) 893-894.
28. C.W. Abney, J.C. Gilhula, K. Lu, et al. Metal-Organic Framework Templated Inorganic Sorbents for Rapid and Effi cient Extraction of Heavy Metals. Adv. Mater., 26 (2014) 7993-7997.
29. C.M. Sun, F. Ma, G.H. Zhang, R.J. Qu, et al. Removal of Mercury Ions from Ethanol Solution Using Silica Gel Functionalized with Amino-Terminated Dendrimer-Like Polyamidoamine Polymers: Kinetics and Equilibrium Studies, J. Chem. Eng. Data, 56 (2011) 4407-4415.
30. J.D. Xiao, L.G. Qiu, X. Jiang, et al. Magnetic porous carbons with high adsorption capacity synthesized by a microwave-enhanced high temperature ionothermal method from a Fe-based metal-organic framework. Carbon, 59 (2013) 372-382.
31. M.A. Farajzadeh, A.B. Monji. Adsorption characteristics of wheat bran towards heavy metal cations. Sep. Purif. Technol., 38 (2004) 197-207.
32. M. Kumar, B.P. Tripathi, V.K. Shahi, Crosslinked chitosan/polyvinyl alcohol blend beads for removal and recovery of Cd(II) from wastewater. J. Hazard. Mater., 172 (2009) 1041-1048.
33. A. Ozer, H.B. Pirincci, The adsorption of Cd(II) ions on sulphuric acid-treated wheat bran. J. Hazard. Mater., 137 (2006) 849-855.
34. V.N. Tirtom, A. Dinçer, S. Becerik, et al. Comparative adsorption of Ni(II) and Cd(II) ions on epichlorohydrin crosslinked chitosan-clay composite beads in aqueous solution, Chem. Eng. J., 197 (2012) 379-386.